

International Journal of Modern Physics A  
 © World Scientific Publishing Company

## LARGE-ANGLE NON-GAUSSIANITY IN SIMULATED HIGH-RESOLUTION CMB MAPS

ARMANDO BERNUI

*Instituto de Ciências Exatas, Universidade Federal de Itajubá,  
 37500-903 Itajubá – MG, Brazil*

MARCELO J. REBOUÇAS AND ANTONIO F. F. TEIXEIRA

*Centro Brasileiro de Pesquisas Físicas  
 Rua Dr. Xavier Sigaud 150, 22290-180 Rio de Janeiro – RJ, Brazil*

Received Day Month Year

Revised Day Month Year

A detection or nondetection of primordial non-Gaussianity by using the cosmic microwave background radiation (CMB) offers a way of discriminating inflationary scenarios and testing alternative models of the early universe. This has motivated the considerable effort that has recently gone into the study of theoretical features of primordial non-Gaussianity and its detection in CMB data. Among such attempts to detect non-Gaussianity, there is a procedure that is based upon two indicators constructed from the skewness and kurtosis of large-angle patches of CMB maps, which have been proposed and used to study deviation from Gaussianity in the WMAP data (see Refs. 1 and 2). Simulated CMB maps equipped with realistic primordial non-Gaussianity are essential tools to test the viability of non-Gaussian indicators in practice, and also to understand the effect of systematics, foregrounds and other contaminants. In this work we extend and complement the results Refs. 1 and 2 by performing an analysis of non-Gaussianity of the high-angular resolution simulated CMB temperature maps endowed with non-Gaussianity of the local type, for which the level of non-Gaussianity is characterized by the dimensionless parameter  $f_{NL}^{\text{local}}$ .

*Keywords:* Non-Gaussianity; cosmic microwave background radiation; inflation.

PACS numbers: 98.80.Es, 98.70.Vc, 98.80.-k

### 1. Introduction

The statistical properties of the temperature anisotropies of cosmic microwave background (CMB) radiation offer a powerful probe of the physics of the primordial universe. In particular the study of non-Gaussianity of CMB is a powerful approach to probe the origin and evolution of structures in the universe (see, for example, the Refs. 3–5 and references therein). Given the far reaching consequences of a convincing detection (or non-detection) of primordial non-Gaussianity for our description of the physics of the early universe, it is important to employ different statistical tools to quantify its amount, type and the angular scale in order to have information

2 *Armando Bernui, Marcelo J. Rebouças & Antonio F. F. Teixeira*

that may be helpful for identifying its causes. Apart from revealing features of non-Gaussianity, different statistical estimators can be sensitive to different systematics. On the other hand, since one does not expect that a single statistical estimator can be sensitive to all possible forms of non-Gaussianity that may be present in CMB data, it is important to study the possible deviations from Gaussianity by using different statistical tools to identify any non-Gaussian signals in the CMB data.

Recent analyses of CMB data made with different statistical tools have provided indications of either consistency or deviation from Gaussianity (see, e.g., Ref. ?). In a recent paper<sup>1</sup> we have proposed two new large-angle non-Gaussianity indicators, based on skewness and kurtosis of large-angle patches of CMB maps, which provide measures of the departure from Gaussianity on large angular scales. We have used these indicators to carry out analyses of large-angle deviation from Gaussianity in both band and foreground-reduced WMAP CMB maps with and without a *KQ75* mask.<sup>1,2</sup> We found that while non-Gaussianity of the Q, V, and W masked maps are consistent with Gaussianity, there is a strong indication of deviation from Gaussianity in the K and Ka masked maps. We have also shown that the full-sky five-year foreground-reduced internal linear combination (ILC)<sup>17,18</sup> as well as the harmonic ILC (HILC)<sup>19</sup> and the needlet ILC (NILC)<sup>20</sup> maps present a significant deviation from Gaussianity.<sup>2</sup>

Simulated CMB maps endowed with assigned primordial non-Gaussianity are essential tools to test the power and sensitivity of non-Gaussian indicators. The first reported simulations of CMB temperature maps with primordial non-Gaussianity introduced through a non-Gaussian parameter  $f_{\text{NL}}$  were given by the WMAP team.<sup>21</sup> Subsequently, Liguori et al. produced generalized algorithm that improves the computational speed and accuracy,<sup>22</sup> and includes polarization.<sup>23</sup> A set of 300 temperature and polarization maps with non-Gaussianities of the local type at the WMAP angular resolution were then produced.<sup>23</sup> More recently, Elsner and Wandelt<sup>24</sup> presented new algorithm and generated 1 000 high-angular resolution simulated non-Gaussian CMB temperature and polarization maps with non-Gaussianities of the local type, for which the level of non-Gaussianity is defined by the dimensionless parameter  $f_{\text{NL}}^{\text{local}}$ .

In this paper, we extend and complement the investigations of Refs.1 and 2 (see also the related Ref. 25), by using their skewness and kurtosis indicators to carry out analyses of Gaussianity of high-angular resolution simulated non-Gaussian CMB temperature maps, equipped with non-Gaussianity of local type with different amplitude parameters  $f_{\text{NL}}^{\text{local}}$ , and generated according to the procedure given by Elsner and Wandelt<sup>24</sup>.

The structure of the paper is as follows. In Sec. 2 we introduce our non-Gaussianity indicators. Section 3 contains the results of applying our statistical indicators to the non-Gaussian simulated maps and our main conclusions.

## 2. Indicators and Maps of Non-Gaussianity

The steps of a constructive way of defining our non-Gaussianity indicators  $S$  and  $K$ , and the associated maps (discrete functions defined on  $S^2$ ) from input CMB (simulated or real data) maps are the following:<sup>1,2</sup>

- i. Take a discrete finite set of points  $\{j = 1, \dots, N_c\}$  homogeneously distributed on the CMB celestial sphere  $S^2$  as the centers of spherical caps of a given aperture  $\gamma$ ; and calculate for each cap  $j$  the skewness and kurtosis given, respectively, by

$$S_j \equiv \frac{1}{N_p \sigma_j^3} \sum_{i=1}^{N_p} (T_i - \overline{T}_j)^3 \quad \text{and} \quad K_j \equiv \frac{1}{N_p \sigma_j^4} \sum_{i=1}^{N_p} (T_i - \overline{T}_j)^4 - 3, \quad (1)$$

where  $N_p$  is the number of pixels in the  $j^{\text{th}}$  cap,  $T_i$  is the temperature at the  $i^{\text{th}}$  pixel,  $\overline{T}_j$  is the CMB mean temperature of the  $j^{\text{th}}$  cap, and  $\sigma$  is the standard deviation. Clearly, the whole set of numbers  $S_j$  and  $K_j$  for each  $j$ , obtained through this discrete scanning of the CMB sphere, can be viewed as a measure of non-Gaussianity in the direction of the center of the cap centered at  $(\theta_j, \phi_j)$  with aperture  $\gamma$ .

- ii. Patching together the  $S_j$  and  $K_j$  values for all spherical cap  $j$ , give discrete functions  $S = S(\theta, \phi)$  and  $K = K(\theta, \phi)$  defined over the celestial sphere, which can be used to measure the deviation from Gaussianity as a function of the angular coordinates  $(\theta, \phi)$ . The Mollweide projection of skewness and kurtosis functions  $S = S(\theta, \phi)$  and  $K = K(\theta, \phi)$  are nothing but skewness and kurtosis maps, hereafter referred to as  $S$ -map and  $K$ -map, respectively.

Clearly, the functions  $S = S(\theta, \phi)$  and  $K = K(\theta, \phi)$  are functions defined on  $S^2$  and can be expanded into their spherical harmonics to have their power spectra  $S_\ell$  and  $K_\ell$ . Thus, for example, for the kurtosis indicator  $K = K(\theta, \phi)$  one has

$$K(\theta, \phi) = \sum_{\ell=0}^{\infty} \sum_{m=-\ell}^{\ell} b_{\ell m} Y_{\ell m}(\theta, \phi), \quad (2)$$

and can calculate the corresponding angular power spectrum

$$K_\ell = \frac{1}{2\ell + 1} \sum_m |b_{\ell m}|^2, \quad (3)$$

which can be used to quantify the amplitude (level) and angular scale of the deviation from Gaussianity. The power spectrum can also be used to calculate the statistical significance of such deviation by comparison with the corresponding power spectrum calculated from input Gaussian maps ( $f_{\text{NL}}^{\text{local}} = 0$ ). Obviously, similar expressions and analyses of the statistical significance can be made for the skewness  $S = S(\theta, \phi)$ .

In the next section we shall use the statistical indicators  $S = S(\theta, \phi)$  and  $K = K(\theta, \phi)$  to make analyses of non-Gaussianity of the high-angular resolution simulated CMB temperature maps endowed with non-Gaussianities of the local

4 *Armando Bernui, Marcelo J. Rebouças & Antonio F. F. Teixeira*

type, for which the level of non-Gaussianity is characterized by the dimensionless parameter  $f_{\text{NL}}^{\text{local}}$ .

### 3. Main Results and Conclusions

From the previous section it is clear that in order to calculate the skewness and kurtosis functions  $S = S(\theta, \phi)$  and  $K = K(\theta, \phi)$  and the associated  $S$  and  $K$  maps, one ought to have an input CMB map. The input maps used in our analyses are high-angular resolution simulated CMB temperature maps endowed with non-Gaussianities of the local type defined by different values of the dimensionless amplitude parameter  $f_{\text{NL}}^{\text{local}}$ .

A simulated map with a desired level of non-Gaussianity  $f_{\text{NL}}^{\text{local}}$  is such that the spherical harmonic coefficients are given by<sup>24</sup>

$$a_{\ell m} = a_{\ell m}^{\text{L}} + f_{\text{NL}}^{\text{local}} \cdot a_{\ell m}^{\text{NL}}, \quad (4)$$

where  $a_{\ell m}^{\text{L}}$  and  $a_{\ell m}^{\text{NL}}$  are the linear and non-linear spherical harmonic coefficients of the simulated CMB non-Gaussian maps generated in Ref. 24 and are available for download.<sup>a</sup>

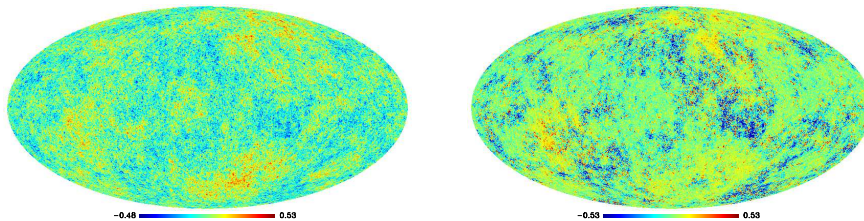


Fig. 1. Simulated CMB temperature fluctuations maps. The left panel shows a Gaussian map ( $f_{\text{NL}}^{\text{local}} = 0$ ) while the right panel depicts a non-Gaussian map generated with  $f_{\text{NL}}^{\text{local}} = 5000$ . We have taken this value for  $f_{\text{NL}}$  just as an example that makes the non-Gaussian effects visible by naked eye through the comparison between the Gaussian and non-Gaussian maps. Temperatures are in  $mK$ .

Figure 1 shows examples of such simulated input CMB maps. The left panel gives a Gaussian map  $f_{\text{NL}}^{\text{local}} = 0$ , while the right panel shows a non-Gaussian maps with  $f_{\text{NL}}^{\text{local}} = 5000$ . The HEALPix resolution parameter for map of Fig. 1, as well as in all the high resolution simulated input CMB maps used in this paper, is  $N_{\text{side}} = 512$ , which corresponds to 3 145 728 pixels. A maximum multipole moment  $\ell_{\text{max}} = 1024$  was also taken.

In the following we report the results of our analyses made by using 1 000 simulated as input CMB temperature maps endowed with non-Gaussianities of the local type with amplitude parameter  $f_{\text{NL}}^{\text{local}} = 0, 100, 1000, 3000$ .

In our calculations of skewness and kurtosis indicator maps ( $S$ -map and  $K$ -map), to minimize the statistical noise we have scanned the celestial sphere

<sup>a</sup> <http://planck.mpa-garching.mpg.de/cmb/fnl-simulations>.

with spherical caps of aperture  $\gamma = 90^\circ$ , centered at  $N_c = 3072$  points on the two-sphere homogeneously generated by using HEALPix package.<sup>27</sup>

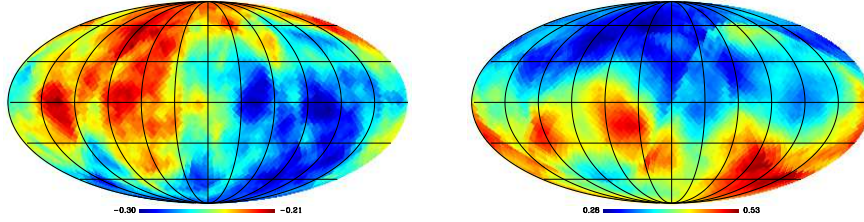


Fig. 2. Skewness (left) and kurtosis (right) maps calculated from input simulated maps with  $f_{\text{NL}}^{\text{local}} = 1000$ . Clearly, according to Eq.1 the values in both  $S$  and  $K$  are dimensionless numbers.

As an illustration of typical skewness and kurtosis maps, Fig. 2 shows the Mollweide projection of  $S$  (left) and  $K$  (right) maps generated from an input CMB simulated map for  $f_{\text{NL}}^{\text{local}} = 1000$ . These maps show spots with higher and lower values of  $S(\theta, \phi)$  and  $K(\theta, \phi)$ , which suggest *large-angle* dominant components (low  $\ell$ ) in these maps. We have also calculated similar maps from the simulated input maps endowed with non-Gaussianity of local type for the other values of  $f_{\text{NL}}^{\text{local}}$  that we are concerned with in this paper. However, since these maps provide only *qualitative* information, to avoid repetition we only depict the pair of maps of Figs. 2 merely for illustrative purpose.

In order to obtain *quantitative* large-angle-scale information of the non-Gaussianity of 4000 calculated  $S$  and  $K$  maps (obtained from  $4 \times 1000$  simulated input CMB maps generated for  $f_{\text{NL}}^{\text{local}} = 0, 100, 1000, 3000$ ), we have calculated the low  $\ell$  ( $\ell = 1, \dots, 10$ ) averaged power spectra  $S_\ell$  and  $K_\ell$ , obtained by averaging over 1000 power spectra of  $S$  and  $K$  maps, calculated for each value of  $f_{\text{NL}}^{\text{local}}$ . The statistical significance of these power spectra is estimated by comparing the values of  $S_\ell$  and  $K_\ell$  obtained from input maps generated for  $f_{\text{NL}}^{\text{local}} = 100, 1000, 3000$  with the values of the corresponding power spectra  $S_\ell$  and  $K_\ell$  obtained from the Gaussian ( $f_{\text{NL}}^{\text{local}} = 0$ ) input simulated map.

Figure 3 shows the average power spectra of the skewness  $S_\ell$  (left panel) and kurtosis  $K_\ell$  (right panel), for  $\ell = 1, \dots, 10$ , calculated from input simulated Gaussian ( $f_{\text{NL}}^{\text{local}} = 0$ ) maps, and from CMB maps equipped with non-Gaussianity of the local type for which  $f_{\text{NL}}^{\text{local}} = 100, 1000, 3000$ . The 95% confidence level, obtained from the  $S$  and  $K$  maps calculated from the Gaussian CMB simulated maps, is indicated in this figure by the dashed line.<sup>b</sup>

To the extent that the average  $S_\ell$  and  $K_\ell$  obtained from input simulated CMB maps endowed with  $f_{\text{NL}}^{\text{local}} = 100$  are within 95% Monte-Carlo (MC) average values of  $S_\ell$  and  $K_\ell$  for  $f_{\text{NL}}^{\text{local}} = 0$ , Fig. 3 shows that our indicators are not suitable to

<sup>b</sup>For more details on the calculation of  $S$  and  $K$  maps and associated power spectra we refer the readers to Refs. 1 and 2.

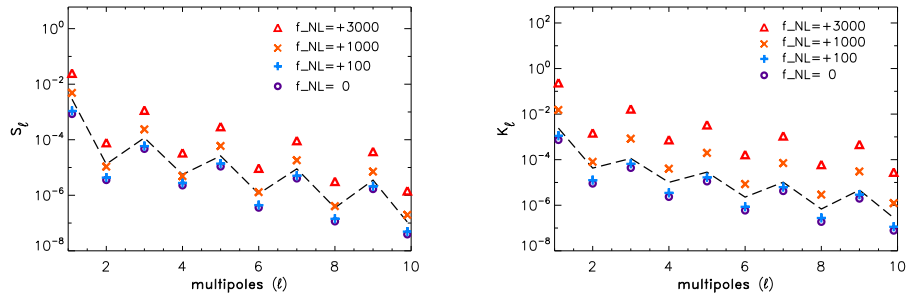
6 *Armando Bernui, Marcelo J. Rebouças & Antonio F. F. Teixeira*

Fig. 3. Low  $\ell$  average power spectra of skewness  $S_\ell$  (left) and kurtosis (right)  $K_\ell$  calculated from the Gaussian ( $f_{\text{NL}}^{\text{local}} = 0$ ) and non-Gaussian ( $f_{\text{NL}}^{\text{local}} \neq 0$ ) input simulated CMB maps. The 95% confidence level relative to the Gaussian maps is indicated by the dashed line.

detect this small level of primordial non-Gaussianity of local type in CMB maps. However, this figure also shows that they can be effectively employed to detect higher level of non-Gaussianity of local type. These results square with the refined numerical analysis we shall report in the remainder of this paper.

To have an overall assessment power spectra  $S_\ell$  and  $K_\ell$ , calculated from the input simulated non-Gaussian maps equipped primordial non-Gaussianity of local type, we have performed a  $\chi^2$  test to find out the goodness of fit for  $S_\ell$  and  $K_\ell$  multipole values as compared to the expected multipole values obtained from  $S$  and  $K$  maps calculated from Monte-Carlo (MC) statistically Gaussian ( $f_{\text{NL}}^{\text{local}} = 0$ ) simulated CMB maps. In each case, this gives a number that quantifies collectively the deviation from Gaussianity. For the power spectra  $S_\ell$  and  $K_\ell$  we found the values given in Table 1 for the ratio  $\chi^2/\text{dof}$  (dof stands for degrees of freedom) for the power spectra calculated from non-Gaussianity of local type with  $f_{\text{NL}}^{\text{local}} = 100, 1000, 3000$ .

Table 1.  $\chi^2$  test goodness of fit for  $S_\ell$  and  $K_\ell$  calculated from the maps with different level of non-Gaussianity as compared with the corresponding expected values obtained from MC simulated CMB input maps with  $f_{\text{NL}}^{\text{local}} = 0$ .

Level of non-Gaussianity	$\chi^2$ for $S_\ell$	$\chi^2$ for $K_\ell$
$f_{\text{NL}}^{\text{local}} = 100$	$4.00 \times 10^{-3}$	$3.10 \times 10^{-2}$
$f_{\text{NL}}^{\text{local}} = 1000$	$3.02 \times 10$	$5.50 \times 10^2$
$f_{\text{NL}}^{\text{local}} = 3000$	$1.52 \times 10^3$	$1.98 \times 10^5$

Clearly, the greater are the values for  $\chi^2/\text{dof}$  the smaller are the  $\chi^2$  probabilities, that is the probability that the values of power spectra  $S_\ell$  and  $K_\ell$  and the expected values of the power spectra of the Gaussian maps agree. Thus, from Table 1 one concludes that the maps endowed with  $f_{\text{NL}}^{\text{local}} = 100$  present very small level of primordial non-Gaussianity, as detected by our indicators, while the non-Gaussianity

of the maps with  $f_{\text{NL}}^{\text{local}} = 1000$  and  $3000$  are a few orders of magnitude higher and suitably detected by both indicators  $S$  and  $K$ , in particular by the kurtosis indicator  $K$ .

### Acknowledgments

M.J. Rebouças acknowledges the support of FAPERJ under a CNE E-26/101.556/2010 grant. This work was also supported by Conselho Nacional de Desenvolvimento Científico e Tecnológico (CNPq) - Brasil, under grant No. 475262/2010-7. A.B. was partially supported by FAPEMIG under grant APQ-01893-10. A.B. and M.J.R. thank CNPq for the grants under which this work was carried out. We acknowledge use of the simulated maps made available by Elsner and Wandelt<sup>24</sup> and the HEALPix package.<sup>27</sup>

### References

1. A. Bernui and M. J. Rebouças, *Phys. Rev. D* **79**, 063528 (2009).
2. A. Bernui and M. J. Rebouças, *Phys. Rev. D* **81**, 063533 (2010).
3. E. Komatsu, *Class. Quant. Grav.* **27**, 124010 (2010).
4. M. Liguori, E. Sefusatti, J. R. Fergusson and E. P. S. Shellard, *Adv. Astron.* **2010**, 980523 (2010).
5. Xingang Chen, *Adv. Astron.* **2010**, 638979 (2010).
6. E. Komatsu et al., *Astrophys. J. Suppl.* **148**, 119 (2003); D. N. Spergel et al., *Astrophys. J. Suppl.* **170**, 377 (2007); P. Vielva, E. Martínez-González, R. B. Barreiro, J. L. Sanz and L. Cayón, *Astrophys. J.* **609**, 22 (2004); M. Cruz, E. Martínez-González, P. Vielva and L. Cayón, *Mon. Not. R. Astron. Soc.* **356**, 29 (2005);
7. M. Cruz, L. Cayón, E. Martínez-González, P. Vielva and J. Jin, *Astrophys. J.* **655**, 11 (2007); A. Bernui, B. Mota, M. J. Rebouças and R. Tavakol, *Int. J. Mod. Phys. D* **16**, 411 (2007); C. Raeth P. Schuecker and A. J. Banday, *Phys. Rev. Lett.* **102**, 131301 (2009); A. Bernui, B. Mota, M. J. Rebouças and R. Tavakol, *Astron. & Astrophys.* **464**, 479 (2007);
8. C. Raeth, P. Schuecker and A. J. Banday, *Mon. Not. R. Astron. Soc.* **380**, 466 (2007); L. Cayón, J. Jin and A. Treaster, *Mon. Not. R. Astron. Soc.* **362**, 826 (2005); Lung-Y Chiang and P. D. Naselsky, *Int. J. Mod. Phys. D* **15**, 1283 (2006); J. D. McEwen, M. P. Hobson, A. N. Lasenby and D. J. Mortlock, *Mon. Not. R. Astron. Soc.* **371**, L50 (2006);
9. J. D. McEwen, M.P. Hobson, A. N. Lasenby and D. J. Mortlock, *Mon. Not. R. Astron. Soc.* **388**, 659 (2008); A. Bernui, C. Tsallis and T. Villela, *Europhys. Lett.* **78**, 19001 (2007); L.-Y. Chiang, P. D. Naselsky and P. Coles, *Astrophys. J.* **664**, 8 (2007); C.-G. Park, *Mon. Not. R. Astron. Soc.* **349**, 313 (2004);
10. H. K. Eriksen, D. I. Novikov, P. B. Lilje, A. J. Banday and K. M. Górski, *Astrophys. J.* **612**, 64 (2004); M. Cruz, M. Tucci, E. Martínez-González and P. Vielva, *Mon. Not. R. Astron. Soc.* **369**, 57 (2006); M. Cruz, N. Turok, P. Vielva, E. Martínez-González and M. Hobson, *Science* **318**, 1612 (2007); P. Mukherjee and Y. Wang, *Astrophys. J.* **613**, 51 (2004);
11. D. Pietrobon, P. Cabella, A. Balbi, G. de Gasperis and N. Vittorio, *Mon. Not. R. Astron. Soc.* **396**, 1682 (2009); D. Pietrobon, P. Cabella, A. Balbi, R. Crittenden, G. de Gasperis and N. Vittorio, *Mon. Not. R. Astron. Soc.* **402**, L34 (2010); P. Vielva and J. L. Sanz, *Mon. Not. R. Astron. Soc.* **397**, 837 (2009);

8 *Armando Bernui, Marcelo J. Rebouças & Antonio F. F. Teixeira*

12. B. Lew, *JCAP* **08**, 017 (2008); A. Bernui and M. J. Rebouças, *Int. J. Mod. Phys. A* **24**, 1664 (2009); M. Kawasaki, K. Nakayama, T. Sekiguchi, T. Suyama and F. Takahashi, *JCAP* **11**, 019 (2008); M. Kawasaki, K. Nakayama and F. Takahashi, *JCAP* **01**, 026 (2009);
13. M. Kawasaki, K. Nakayama, T. Sekiguchi, T. Suyama and F. Takahashi, *JCAP* **01**, 042 (2009); M. Cruz, E. Martínez-González and P. Vielva, *The WMAP cold spot*, arXiv:0901.1986 [astro-ph]; A. Bernui, M. J. Rebouças and A. F. F. Teixeira, *Testing large-angle deviation from Gaussianity in CMB maps*, arXiv:1005.0883 [astro-ph.CO]; G. Rossmanith, C. Raeth, A. J. Banday and G. Morfill, *Mon. Not. R. Astron. Soc.* **399**, 1921 (2009);
14. A. Bernui and M. J. Rebouças *Int. J. Mod. Phys. D* **19**, 1411 (2010); A. Bernui, M. J. Rebouças and A. F. F. Teixeira, *Int. J. Mod. Phys. D* **19**, 1405 (2010); C. Raeth, G. Rossmanith, G. Morfill, A. J. Banday and K. M. Górski, *Probing non-Gaussianities on Large Scales in WMAP5 and WMAP7 Data using Surrogates*, arXiv:1005.2481 [astro-ph.CO]; C. Raeth *et al.*, *Scale-dependent non-Gaussianities in the WMAP data as identified by using surrogates and scaling indices*, arXiv:1012.2985 [astro-ph.CO];
15. L. R. Abramo and T. S. Pereira, *Testing gaussianity, homogeneity and isotropy with the cosmic microwave background*, arXiv:1002.3173 [astro-ph.CO]; T. Kahniashvili, G. Lavrelashvili and B. Ratra, *Phys. Rev. D* **78**, 063012 (2008);
16. C. J. Copi, D. Huterer, D. J. Schwarz and G. D. Starkman, *Adv. Astron.* **2010**, 847541 (2010); P. Cabella *et al.*, *Foreground influence on primordial non-Gaussianity estimates: needlet analysis of WMAP 5-year data*, arXiv:0910.4362 [astro-ph.CO];
17. G. Hinshaw *et al.*, *Astrophys. J. Suppl.* **180**, 225 (2009).
18. B. Gold *et al.*, *Astrophys. J. Suppl.* **192**, 15 (2011).
19. J. Kim, P. Naselsky and P. R. Christensen, *Phys. Rev. D* **77**, 103002 (2008).
20. J. Delabrouille *et al.*, *Astron. & Astrophys.* **493**, 835 (2009).
21. E. Komatsu, *et al.*, *Astrophys. J. Suppl.* **148**, 119 (2003).
22. M. Liguori, S. Matarrese and L. Moscardini, *Astrophys. J.* **597**, 57 (2003).
23. M. Liguori, A. Yadav, , F. K. Hansen, E. Komatsu, S. Matarrese and B. Wandelt, *Phys. Rev. D* **76**, 105016 (2007), Erratum: *Phys. Rev. D* **77**, 029902 (2008).
24. F. Elsner and B. D. Wandelt, *Astrophys. J. Suppl.* **184**, 264 (2009).
25. A. Bernui and M. J. Rebouças, *Phys. Rev. D* **85**, 023522 (2012).
26. E. Komatsu *et al.*, *Astrophys. J. Suppl.* **180**, 330 (2009).
27. K. M. Górski, E. Hivon, A. J. Banday, B. D. Wandelt, F. K. Hansen, M. Reinecke and M. Bartelman, *Astrophys. J.* **622**, 759 (2005).